Reprinted from August 1980, Vol. 102, Journal of Pressure Vessel Technology

Analysis of Bolted Joints with Nonlinear Gasket Behavior[1]

Alan I. Soler
Chief Technology Officer
Holtec International

Design methods for full face gaskets in bolted pressure vessel joints have received little attention in the literature. Such gasketed joints play a prominent role in attaching rectangular plan from water boxes to rectangular tubesheets in condenser water boxes. With higher cooling water pressures becoming evident due to cooling tower circuits, the water box-tubesheet structure, and its bolted joint connection requires rigorous analysis for both structural integrity and leak tightness. Although it is well known that gasket material has a highly nonlinear stress strain behavior, very few analyses are available to calculate and evaluate the effect of the nonlinear gasket behavior in a bolted joint connection. In this paper, an approximate method for simultaneously analyzing structural integrity and leak tightness of typical bolted flange connections with nonlinear gasket material is developed. The flange is modeled as an elastic element, the bolt is simulated by a linear spring with bending and extensional resistance, and the gasket is modeled by a series of nonlinear compression springs. A simple nonlinear stress-strain relation for initial loading and unloading of the gasket is developed based on experimental data. The analysis technique employs an incremental procedure which follows the configuration through preloading and pressurization and checks structural integrity and gasket leakage. To illustrate the method, a typical full face gasket and flange construction is studied, and the effect of gasket properties on the final state is investigated. A series of simulation results are obtained which illustrate clearly the effect of gasket prestrain, undersizing of bolts, and wall rotational resistance. Of particular importance is a simulation comparing results obtained using actual nonlinear gasket stress-strain data with results obtained using linear models for the gasket. It is demonstrated that for full face gasket configurations, simulation of the nonlinear behavior is required to achieve accurate results. The procedure developed in this work is ideal for optimization of flange gasket configurations because of its cost effectiveness while simultaneously evaluating the interaction between structural integrity and joint leak tightness.

Introduction

An area of considerable importance in pressure vessel design is establishment of a proper flanged-bolted joint connection insuring both joint structural integrity and joint leak tightness. Most joint analyses to date emphasize structural integrity; joint components are designed to experience service stress levels below a specified value. However, maintenance of some preset stress level does not guarantee leak tightness. It is the purpose of this investigation to present an approach which permits simultaneous evaluation of structural integrity and leak tightness. We realize, at the outset, that to achieve accuracy in predicting leakage, nonlinear behavior of the sealing material should be included in the analysis. However, once nonlinear behavior is included, simple formulae, amenable to hand computation, are general precluded; hence, in this work, we strive to develop an efficient numerical solution procedure which is cost-efficient and can be simply implemented in any design office having computer capability.

The design of bolted flange joints using ASME Code rules [1] is based on work by Waters, et al. [2]. In that work, which considers interaction between flanges only at a ring gasket, it is assumed that the bolt stress develops solely due to preloading, does not change during pressurization, and is a direct tensile stress with no bending component. Using Water's method, bolt stresses under operating conditions cannot be assessed, although current codes do require limits on bolt service stresses. Schneider [3] has pioneered the analysis of two identical flat face flanges with uniform hubs compressing a self-energizing gasket located in line with the pressure vessel wall. Waters and Schneider [4] further extend the solution to include nonidentical mating closure elements. In both of the preceding works, soft O-ring gaskets are considered so that flange seating stresses are presumed negligible. Additional work on flange and bolted joint design is found in the text and bibliography provided by Gill in

[1] Support for this study provided by Ecolaire Condenser, Inc., Lehigh Valley, Pa.

Contributed by the Pressure Vessels and Piping Division and presented at the Pressure Vessels and Piping Conference, San Francisco, California, June 25-29, 1979, of THE AMERICAN SOCIETY OF MECHANICAL ENGINEERS. Manuscript received at ASME Headquarters, August 31, 1978; revised manuscript received December 17, 1979.

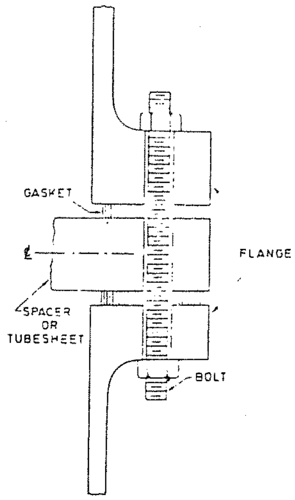

Fig. 1 Bolted joint

reference [5]. It is concluded that, in the design of bolted flange joints, major uncertainties still remain with the gasket behavior and its influence on the overall behavior of the joint. It is in the attempt to simulate the complex behavior of the gasket by an idealized description, and apply the resulting formulation to a real situation, that offers a great challenge to the researcher.

In a recent work, Singh [6] considers the complete analysis of a circular flange-gasket-tubesheet-bolted joint connection as a unit and attempts to predict service stresses in the components, as well as deformations and residual pressures in the gasket (which are a measure of leak tightness). Singh's model considers a gasket inboard of the bolt circle and allows for the possibility of flange contact outside of the bolt circle due to flange rotation. Singh notes that the mathematical model for the gasket presents the greatest problem. A typical spiral wound gasket possesses a highly nonlinear and non-conservative loading, unloading, and reloading characteristic [7]. Further, the minimum surface pressure on the gasket, to maintain a leak-tight joint, depends on surface finish, groove clearance, gasket strip material, loading history, etc. Singh adopts a simplified gasket model in his analysis, assumes that the gasket pressure resultant acts at a known location on the flange (independent of flange flexibility), and also simulates the gasket by a linear elastic spring with different spring rates for loading and unloading. A similar approach, using a much simplified model, is reported by Swick in reference [8].

In this work, we consider analysis of a bolted flange connection having identical flanges, separated by a spacer or tubesheet, and sealed either by a ring gasket inboard of the bolt line, or by full face gaskets. The gasket behavior is presumed to be nonlinear in nature. In order to avoid algebraic excesses, and in order to sharply focus our attention on the formulation and solution procedure, we assume that the spacer or tubesheet elasticity can be ignored. This is a realistic assumption in the case of very thick tubesheets and permits us to deal with only one-half of the flanged joint. Fig. 1 illustrates a typical configuration for the case of a full face gasket which is commonly used in large rectangular condenser water boxes. Both circular flanges and rectangular flanges (such as found in typical power plant condenser water boxes) may be accommodated.

Analysis

Fig. 2 illustrates the flange-gasket model. The bar flange is linearly elastic and is considered as an annular plate section extending over the radial region $-a \leq x \leq b$. Loading and geometric symmetry allows us to focus only on the portion of the plate between two bolt centerlines. The gasket is simulated by nonlinear springs with strain dependent spring rates. For full face gaskets, the gasket springs are positioned over the entire x region; to model ring-type gaskets, inboard of the bolt circle, we simply set spring rates to zero outboard of the region modeling the actual gasket ring. The nonlinear nature of the gasket spring rates suggests the utility of an incremental or rate formulation of the problem coupled with a suitable numerical integration scheme to effect usable solutions.

For the purposes of a simplified analysis, we assume:

1 the rotation of the spacer or tubesheet may be neglected;

2 relatively large diameter flanges such that the flange length $L = a + b$ is much less than the radius of the bolt circle R;

3 the variation of the lateral displacement of the flange between bolt centerlines may be neglected in comparison with the variations in the radial (x) direction.

Nomenclature

a, b, d, L = lengths of various flange parts (Fig. 2)
$w(x)$ = flange elastic deformation
I = moment of inertia of position of flange modelled as elastic strip
x = specifies location on flange
$\dot{w}_o, \dot{\theta}, \dot{\psi}, \dot{\phi}$ = independent rate variables modelling flange deformation rate distribution
$f_2(x), f_3(x)$ = assumed distribution of flange elastic deformation shape
$\dot{F}, \dot{M}$ = applied load and moment rate to inboard edge of flange by internal pressure acting on adjacent shell; $\dot{M}$ may also include flexibility of adjacent shell structure
F_i = current value of load in gasket spring at $x = x_i$
A_{g_i} = plan form area of the gasket region modelled by a spring at $x = x_i$
λ_i = leakage parameter of gasket at $x = x_i$
h_{g_i} = gasket thickness at $x = x_i$
$A_{ij}, \dot{B}_i$ = coefficients in rate equations (equations (2)-(14))
k_B, k_θ = linear springs modelling extensional and rotational elasticity of bolt
k_i = spring rate of gasket region at $x = x_i$
E_B, A_B, I_B, L_B = bolt material and geometric const (equation (15))
k, n = parameters in nonlinear gasket stress strain relation (equation (19))
σ_y = yield stress of bolt material
F_y, M_y = limit load and moment of bolt
α_b = parameter used to incorporate bolt yielding in simulation
h = thickness of elastic flange

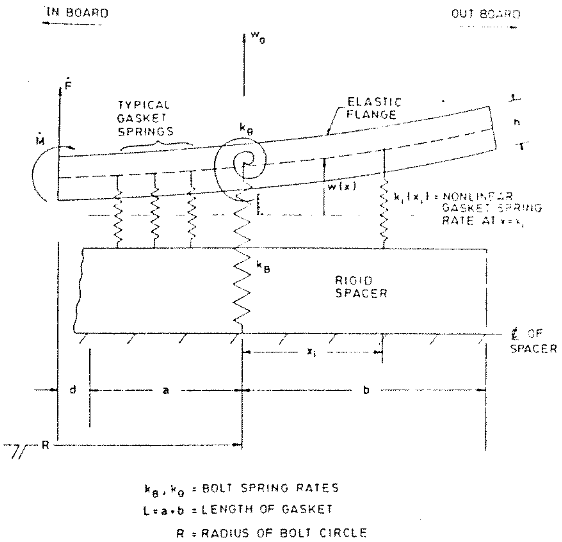

Fig. 2 Flange-gasket model

The foregoing assumptions give sufficient accuracy for our initial investigations, although they may be lifted at the expense of additional computational requirements.

The governing incremental equations for our analysis are obtained by application of the Theorem of Minimum Potential Energy applied to the rate deformation variables of the problem. Since the problem being considered involves only physical nonlinearity (nonlinear gasket material) and retains geometric linearity, it can be easily demonstrated (see Biot [9]) that a variational principle for the deformations can be carried directly over to a variational principle for the velocities in a quasi-static process.

Therefore, if we let $\dot{w}(x)$ represent the rate of change of flange lateral displacement with respect to time or load; then an energy formulation of the problem is given by

$$\delta \int_{-a}^{b} \frac{EI}{2} \left\{ \left(\frac{d^2 \dot{w}}{dx^2} \right)^2 + \frac{1}{R^2} \left(\frac{d\dot{w}}{dx} \right)^2 + \frac{2v}{R} \frac{d\dot{w}}{dx} \frac{d^2 \dot{w}}{dx^2} \right\} dx + \delta U_s = \delta W_e \quad (1)$$

where R is taken as the bolt circle radius, and the flange moment of inertia, between bolt centerlines, is given as

$$I \cong \bar{w} h^3 / 12(1-\nu^2) \quad (2)$$

with $\bar{w}$ equal to the peripheral distance between any two bolt centers. δU_s is the variation of the incremental strain energy of the gasket and bolt expressed in terms of rate variables, and δW_e represents the virtual rate of work done by the incremental external forces acting on the flange.

Using Fig. 2, we assume flange lateral deformation rate in the form

$$\dot{w}(x) = \dot{w}_o + x\dot{\theta} + f_2(x)\dot{\psi} + f_3(x)\dot{\phi} \quad (3)$$

where

$$f_2(x) = \frac{x^2}{2L} + \frac{ax}{L};\ f_3(x) = \frac{x^3}{3L^2} - \frac{xa^2}{L^2};\ L = a + b \quad (4)$$

$\dot{w}_o$ is the current rate of bolt extension, $\dot{\theta}$ is the current rate of flange rotation at $x = -a$, and $\dot{\psi}$, $\dot{\phi}$ are additional rate variables associated with the assumed elastic beam-type deformation modes. We define k_b, k_θ as linear spring rates of the bolt in extension and bending, respectively; similarly, k_i is the current spring rate of the gasket nonlinear spring element centered at x_i. Using the defined spring rates together with equations (3) and (4) yields the energy term U_s in the form

$$U_s = \frac{1}{2} k_b (\dot{w}_o + \dot{\Delta})^2 + \frac{1}{2} k_\theta \left(\dot{\theta} + \frac{a}{L} \dot{\psi} - \frac{a^2}{L^2} \dot{\phi} \right)^2 + \sum_{i=1}^{n} \frac{k_i}{2} (\dot{w}_o + x_i \dot{\theta} + f_2(x_i)\dot{\psi} + f_3(x_i)\dot{\phi})^2 \quad (5)$$

where $\dot{\Delta}$ is a bolt displacement rate applied during the initial phase of the simulation to preload the gasket.

The contribution of the term δW_e is written in the form

$$\delta W_e = \dot{F}[\delta \dot{w}_o - a\delta\dot{\theta} + f_2(-a)\delta\dot{\psi} + f_3(-a)\delta\dot{\phi}] + (\dot{M} - \dot{F}d)\delta\dot{\theta} + \delta W_2 \quad (6)$$

where $\dot{F}$, $\dot{M}$ are loadings applied to the flange by the adjacent structure, and by the effects of pressurization. We restrict $\dot{F}$, $\dot{M}$ to have the form

$$\dot{F} = \dot{p}A;\ \dot{M} = -C\dot{\theta} + \dot{p}Al \quad (p = \text{current pressure}) \quad (7)$$

where A, l are constants to be specified for a particular simulation, and C is a measure of the rotational resistance of the adjacent shell or channel structure. The term δW_2 represents the contribution of incremental pressure forces at locations x_i, subsequent to gasket leakage at x_i. Leakage at any gasket spring location x_i is presumed to occur whenever the following relation is satisfied:

$$|F_i| \leq pA_{gi} \quad (8)$$

$F_i \leq 0$ is the current value of the load in the i^{th} gasket spring, p is the current value of the pressure to be sealed, and A_{gi} is the plan form gasket area modelled at the i^{th} location. For full face gaskets, a failure of the flange due to leakage is assumed to occur when all gasket springs in the region $-a \leq x \leq 0$ satisfy equation (8). For ring-type gaskets inboard of the bolt line, modelled by a single nonlinear spring element, leakage occurs as soon as equation (8) is satisfied for the single spring element.

Note that equation (8) implicitly assumes a gasket seating factor equal to unity. This follows from an assumption of an elastometric gasket material. For asbestos based baskets, equation (8) would require inclusion of an appropriate seating factor. A measure of the sealing of each gasket spring is given by λ_1 defined by

$$\lambda_i = \frac{1}{2} \left\{ 1 + \frac{F_i + pA_{gi}}{|F_i + pA_{gi}|} \right\} \quad (9)$$

Then $\lambda_i = 0$ for $-F_i > pA_{gi}$, and $\lambda_i = 1$ for $-F_i < pA_{gi}$. The virtual rate of work expression δW_2 can then be written in the form

$$\delta W_2 = \dot{p} \sum_{i=1}^{N} A_{gi} \lambda_i [\delta \dot{w}_o + x_i \delta\dot{\theta} + f_2(x_i)\delta\dot{\psi} + f_3(x_i)\delta\dot{\phi}] \quad (10)$$

Applying the variational procedure to equation (5), and using the result, together with equations (6), (7) and (10) in equation (1), yields a relation of the form

$$X_1 \delta\dot{w}_o + X_2 \delta\dot{\theta} + X_3 \delta\dot{\psi} + X_4 \delta\dot{\phi} = 0 \quad (11)$$

As the variations $\delta\dot{w}_o$, $\delta\dot{\theta}$, $\delta\dot{\psi}$, $\delta\dot{\phi}$ are presumed independent, equation (11) yields equations for the current values of the rate variables:

$$\sum_{j=1}^{4} A_{ij} \dot{q}_j = \dot{B}_i \qquad i = 1, 4$$

$$\dot{q}_1 = \dot{w}_o, \dot{q}_2 = \dot{\theta}, \dot{q}_3 = \dot{\psi}, \dot{q}_4 = \dot{\phi} \quad (12)$$

The coefficients appearing in equation (12) are functions of the instantaneous configuration, and change at each step in the loading process. The coefficients A_{ij}, $\dot{B}_i$ have the form

$$\begin{aligned} A_{11} &= k_B + \Sigma k_i;\ A_{12} = A_{21} = \Sigma x_i k_i \\ A_{13} &= A_{31} = \Sigma k_i f_2(x_i);\ A_{14} = A_{41} = \Sigma k_i f_3(x_i) \\ A_{22} &= k_\theta + C + \Sigma k_i x_i^2 \\ A_{23} &= A_{32} = \frac{a}{L} k_\theta + \Sigma k_i x_i f_2(x_i) \end{aligned} \quad (13)$$

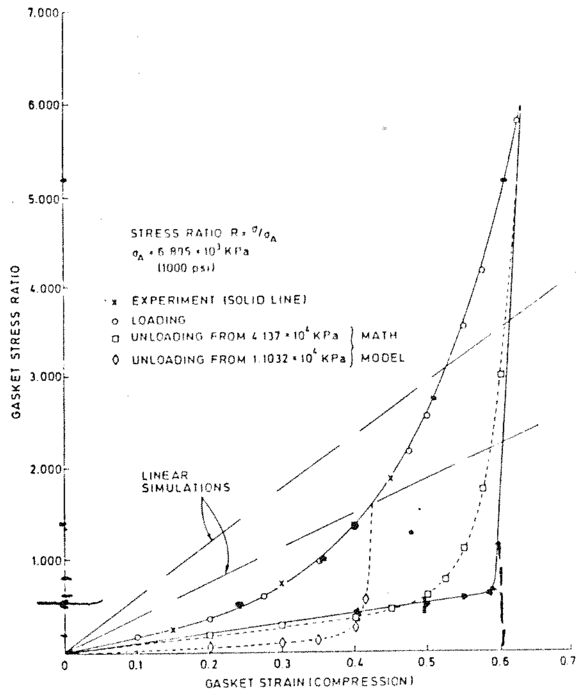

Fig. 3 Neoprene gasket stress-strain relation

$$A_{24} = A_{42} = -\left(\frac{a}{L}\right)^2 k_\theta + \Sigma k_i x_i f_3(x_i)$$

$$A_{33} = EI/L + \frac{a^2}{L^2} k_\theta + \Sigma k_i f_2^{\,2}(x_i)$$

$$A_{34} = A_{43} = EI(b-a)/L^2 - \left(\frac{a}{L}\right)^3 k_\theta + \Sigma k_i f_2(x_2) f_3(x_i)$$

$$A_{44} = 4EI(b^3+a^3)/3L^4 + \left(\frac{a}{L}\right)^4 k_\theta + \Sigma k_i f_3^{\,2}(x_i)$$

$$\begin{aligned} \dot{B}_1 &= \dot{p}A(1+\Sigma\lambda_i A_{gi}/A) + k_B\dot{\Delta} \\ \dot{B}_2 &= \dot{p}A(l-[a+d]+\Sigma\lambda_i x_i A_{gi}/A) \\ \dot{B}_3 &= \dot{p}A(f_2(-a)+\Sigma\lambda_i A_{gi} f_2(x_i)/A) \\ \dot{B}_4 &= \dot{p}A(f_3(-a)+\Sigma\lambda_i A_{gi} f_3(x_i)/A) \end{aligned} \tag{14}$$

In equation (13), (14), the summations extend over all of the gasket springs. Equations (12) - (14) are solved to find the flange deformation as a function of the applied loadings by employing a suitable numerical integration scheme to determine the configuration state at $t+\Delta t$, knowing the configuration state at t. At each stage in the process, the coefficients A_{ij}, $\dot{B}_i$ are computed using the current values of the variables and the current rates $\dot{q}_i$ determined algebraically. The determined $\dot{q}$ variables lead directly to a determination of the new state at the time $t+\Delta t$. The loading consists initially of a specified bolt displacement rate $\dot{\Delta}$ sufficient to impose a compressive load distribution in the gasket springs, together with a balancing loading in the bolt. Subsequently, an appropriate pressurization rate $\dot{p}$ is applied, while holding the bolt preload, until the desired pressure is obtained. Integrity of the flange-gasket configuration is ascertained by consideration of flange and bolt stress, and by monitoring progression of "leakage" along the gasket springs toward the bolt line.

Prior to applying the foregoing simulation, we specify the spring rates used in the formulation of the problem. The linear spring rates k_B, k_θ for the bolt are given as

$$k_B = E_B A_B / L_B; \quad k_\theta = E_B I_B / L_B \tag{15}$$

where L_B, E_B, A_B, I_B are the bolt elastic length, Young's modulus, tensile stress area, and metal moment of inertia, respectively. The spring rates for the nonlinear gasket are discussed in the following section.

Simulation of Nonlinear Gasket Behavior

The solution procedure proposed herein requires that each gasket spring be represented by an incremental force-deformation rate expression of the form

$$\dot{F}_i = K_i \dot{\delta}_i \tag{16}$$

where $\dot{F}_i$ is the rate of change of force in the nonlinear spring element and $\dot{\delta}_i$ is the rate of change of spring length from its unloaded position. The value of K_i is assumed to be a function of the current deformation δ_i. Equation (16) implies that the general computer code is applicable to gasket materials which, during a single cycle of loading and unloading, can be represented by a nonlinear stress strain curve which can effectively be put in the form

$$\dot{\sigma} = E_g \dot{\epsilon} \tag{17}$$

$\dot{\sigma}$, $\dot{\epsilon}$ being stress and strain rate variables for the gasket material and E_g being the current slope of the nonlinear stress strain curve. For any specific material with a suitable stress strain relation defined by testing, the function E_g is approximated by an analytical formula and related to the spring constant K_i in each region. In this work, we demonstrate the approach using a particular stress strain behavior shown in Fig. 3.

The solid curve in Fig. 3 shows test results for stress-strain behavior during a cycle of loading and unloading for a typical neoprene material used for full face gaskets. During the loading cycle, the behavior is simulated by

$$\begin{aligned} \sigma &= E\epsilon & \epsilon &\le \epsilon_1 \\ \sigma &= \sigma_o e^{\epsilon/\epsilon_1} & \epsilon &\ge \epsilon_1 \; ; \quad \epsilon_1 = (\sigma_o/E)e^{1.0} \end{aligned} \tag{18}$$

To approximate the unloading behavior, starting from a state of stress σ_f, ϵ_f, we assume the relationship

$$\frac{\sigma}{\sigma_f} = \frac{1}{1+k}\left[\frac{\epsilon}{\epsilon_f} + k\left(\frac{\epsilon}{\epsilon_f}\right)^n\right] \tag{19}$$

Equation (19) is essentially a Ramberg-Osgood relationship, with the role of stress and strain interchanged. Equation (19) yields

$$\frac{d\sigma}{d\epsilon} = \frac{\sigma_f}{\epsilon_f}\frac{1}{(1+k)}\left[1 + nk\left(\frac{\epsilon}{\epsilon_f}\right)^{n-1}\right] \tag{20}$$

Evaluating equation (20) at the final loaded state yields n as

$$n = \left\{\frac{(d\sigma/d\epsilon)_f(1+k)}{\sigma_f/\epsilon_f} - 1\right\} \Big/ k \tag{21}$$

Therefore, if $(d\sigma/d\epsilon)_f$ is given, for every σ_f, ϵ_f, then for a specified value of k, the unloading behavior is completely determined. We can show that the stress level at the "knee" of the unloading curve is approximated by

$$\sigma_{\text{knee}} = \sigma_f/(1+k) \tag{22}$$

so that, if we insist, for example, that regardless of σ_f, ϵ_f, we always have $\sigma_{\text{knee}} = 0.1\sigma_f$, then $k = 9$.

In the Appendix, we present further details of a specific simulation using the stress strain curve shown in Fig. 3. In general, a particular simulation of the gasket nonlinearity requires that we use the stress strain data for a cycle of loading and unloading to determine the gasket properties σ_o, ϵ_1, $(d\sigma/d\epsilon)_f$, with k, n chosen to reflect the shape of the unloading curve.

For subsequent use in the simulation of full face gaskets, the following relations hold for the current values of the gasket spring rates

$$k_i = E_g A_{gi}/h_{gi} \quad ; \qquad E_g = d\sigma/d\epsilon$$

$$E_g = E \quad ; \qquad \epsilon \leq \epsilon_1 ; \qquad \dot{\epsilon} > 0$$

$$E_g = \frac{\sigma_o}{\epsilon_1} e^{\epsilon/\epsilon_1} ; \qquad \epsilon > \epsilon_1 ; \qquad \dot{\epsilon} > 0 \tag{23}$$

$$E_g = \frac{\sigma_f}{\epsilon_f(1+k)} \left[1 + nk \left(\frac{\epsilon}{\epsilon_f} \right)^{n-1} \right] ; \epsilon \leq \epsilon_f ; \dot{\epsilon} < 0$$

In the foregoing, $\epsilon > 0$ represents compressive gasket strain, A_{gi} for the gasket is defined in equation (8), and h_{gi} is the gasket "thickness" at the i^{th} location.

On occasion, gasket behavior has been simulated by linear spring rates with different rates for loading and for unloading. The foregoing relations can approximate such behavior by assuming that $\epsilon_1 = 1$, specifying $(d\sigma/d\epsilon)_f$ and taking k to be a large enough value so that leakage will occur (in accordance with the criteria of equation (8)) prior to reaching the "knee" of the unloading curve. Two typical linear simulations of loading behavior are also shown on Fig. 3 for later use in this study.

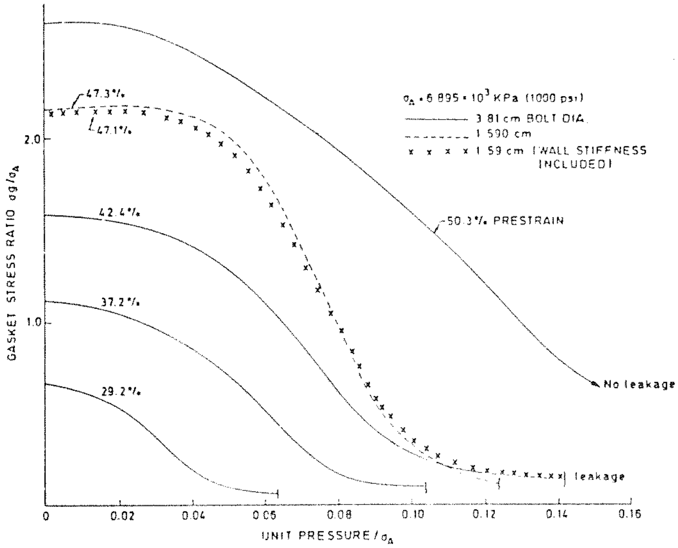

Fig. 4 Gasket pressure versus unit pressure for varying gasket prestrain

Simulation of Bolt Overstress

In the simulation study discussed, the bolt is simulated by a cantilever beam having spring constants in extension k_B and in bending k_θ given by equation (15). As the bolt load and moment are increased during a particular load case, the bolt material may yield causing a reduction in the values of k_B, k_θ in subsequent steps. Since such bolt behavior influences the point at which gasket leakage will be initiated, it is apparent that some attempt should be made to include increased bolt flexibility due to yielding in the numerical simulation. We suggest that the following scheme may be suitable. If the bolt yield stress in simple tension is σ_y, then the maximum direct force F_y to cause bolt yielding in the absence of bending is

$$F_y = \sigma_y A_B \tag{24}$$

Similarly, in the absence of any direct loading, the maximum bending moment to cause first yield is

$$M_y = \sigma_y \frac{\pi}{4} (d_B/2)^3 \tag{25}$$

where d_b is the bolt diameter assumed to support bending. Using equations (24), (25) we introduce the parameter α_b, defined as

$$\alpha_b = 1 - F/F_y - M/M_y \tag{26}$$

where F, M are the current force and bending moment in the bolt. First yield in the bolt occurs when $\alpha_b = 0$. Subsequent to first yield in the bolt, we simulate the increased bolt flexibility by reducing the bolt spring constants in a linear manner as F and M increase further during the simulation. The reduction is accomplished at the rate which requires that both bolt spring constants approach zero as the critical bolt cross section approaches a complete plastic hinge under the combined effect of F and M. It is clear from equation (13) that changes in the values of k_B, k_θ have a possibly significant effect on the flange deformation rate.

We do not pretend that this is an exact model of the bolt behavior subsequent to first yield; it does, however, lend itself to simple implementation in the incremental computer code. Since, for a circular section, the plastic limit moment for a plastic hinge, under pure moment loading, is $1.7\ M_y$, we can show that the following spring constant reduction scheme in the solution procedure will yield the results desired:

$\alpha_b \geq 0$; k_B, k_θ have elastic values

$0 > \alpha_b > -0.412\ M_b/M_y$; k_B, k_θ multiplied by $1 + \alpha_b/(0.412\ M_b/M_y)$ (27)

$-0.412\ M_b/M_y \geq \alpha_b$; k_B, $k_\theta = 0$

The foregoing scheme is a convenient method of effecting reduction in bolt "resistance" due to overstress of the bolt cross section.

Application

A computer code, based on the model discussed in this work and incorporating an incremental solution scheme, has been developed and implemented on the Univac 90/70 at the University of Pennsylvania. Based on an assumed initial bolt loading, the preload stress distribution in the gasket and flange are computed by incrementally applying the bolt load. Subsequent to this initial stage, pressure increments are applied and the equations updated after each step based on the current gasket strain at each location x_i. The solution proceeds until the desired pressure is reached, until the flange or bolt "fails," or until all of the gasket springs, inboard of the bolt line, "leak."

As an example of the simulation, the following full face flange-gasket configuration representative of a strip of the rectangular condenser water box flange in a large power plant, is modelled and subjected to various load cases. The dimensional data is taken from a full-scale design.

Number of gasket springs = 6 (3 inboard of bolt line)
Width of flange strip (center to center bolt spacing) = 8.89 cm (3.5 in.)
Bolt length = 11.43 cm (4.5 in.)
Bolt diameter = 3.81 cm = (1.5 in.)
Flange, bolt modulus = 200 × 10^6 kPa (29 × 10^6 psi)
a (Fig. 2) = 5.08 cm (2 in.)
b (Fig. 2) = 5.715 cm (2.25 in.)
d (Fig. 2) = 0.9525 cm (0.375 in.)
Flange thickness h (Fig. 2) 3.81 cm (1.5 in.)
Maximum desired pressure = 1.034 × 10^3 kPa (150 psi)
Gasket nonlinear properties from equation (21)-(23) and Fig. 3
Gasket thickness = 0.476 cm (0.1875 in.)
Bolt yield stress = 0.724 × 10^6 kPa (105,000 psi)
Flange yield stress = 0.2069 × 10^6 kPa (30,000 psi)

The applied force and moment, F, M are taken as $F/P = 59.9$ (N/kPa), $M/p = 0.979$ (N-m/kPa); the values used are obtained from full-scale test data available to the author. In this initial calculation, we set $C = 0$ in equation (7) implying that the rotational resistance of the adjacent structure is negligible. As this simulation is for a rectangular flange, the bolt circle radius is set to a large number sufficient to eliminate the second and third terms in the integrand of equation (1).

Effect of Initial Preload on Leakage. Fig. 4 shows the results of a series of runs designed to study the effect of initial preload on the leakage pressure. Each curve in Fig. 4 represents a different initial gasket prestrain resulting from bolt preload. Because of flange elasticity, the prestrain indicated for each curve is for the gasket spring just inboard of the bolt line.

For bolt preload sufficient to induce 50.3 percent compressive strain prior to pressurization, the result in Fig. 4 shows that the design pressure is met without any leakage. Although computer output is not presented herein, examination of that output indicates that residual pressure on the gasket spring, nearest the inboard end, is 1.572×10^3 kPa (228 psi) at the final design pressure. At an initial prestrain of 42.4 percent, the system "leaks" at 0.983×10^3 kPa (142.5 psi); the residual pressure on the gasket spring nearest the inboard end reaches chamber pressure (signifying beginning leakage at this spring) at a pressure of 0.837×10^3 kPa (121.5 psi). The remaining curves at 37.2 percent and 29.2 percent prestrain indicate complete leakage of all springs inboard of bolt line at pressures of 0.714×10^3 kPa (103.5 psi) and 0.434×10^3 kPa (63 psi), respectively. In the configuration studied, bolt size is such that the bolt remains elastic throughout the preload and pressurization stages. A summary of the bolt stress level at the end of the preload state, and at the maximum pressurized state obtained is shown in the following table.

Table 1 Bolt stress level

Prestrain, percent	Preload σ_D/σ_A	Preload σ_B/σ_A	Final σ_D/σ_A	Final σ_B/σ_A
50.3	21.61	6.934	23.523	39.304
42.4	13.063	5.267	15.797	58.885
37.2	9.308	4.202	10.898	47.430
29.2	5.579	2.868	6.305	31.869

$$\sigma_A = 6.895 \times 10^3 \text{ kPa (1000 psi)} \quad (30)$$

σ_D = average stress; σ_B = maximum bending stress

It is clear from the table that although the average bolt stress remains relatively constant through the loading program, flange rotation induces considerable bending stress in the bolt. There is a direct consequence of the relatively thin flange used for this low pressure unit. It is of interest to note that for these runs, the flange "pivot point" during pressurization is at or outboard of the bolt line. The pivot point is defined, herein, as the location of the demarcation between relaxation of gasket loading and continued gasket compression as the unit pressure is increased.

Effect of Bolt Overstress on Leakage. To demonstrate the effect of bolt overstress, we consider the same geometry and loading but reduce the bolt diameter to 1.5875 cm (0.625 in.). The initial percent prestrain is established at 47.3 percent with a resulting bolt stress ratio

$$\sigma_D/\sigma_A = 100.84 \qquad \sigma_B/\sigma_A = 2.775$$

Note that the bolt is almost at first yield just due to prestrain. The result of this run is also shown on Fig. 4. At a pressure of 124 kPa (18 psi), the bolt spring constants k_b, k_θ are set to zero in accordance with the criteria set forth in this paper (equation (27)). It is seen that flange rotations increase dramatically as pressure rises; the gasket pressure falls significantly more rapidly in this case when the bolt resistance to extension and rotation falls to zero. Final failure is by leakage at 848 kPa (123 psi). It is of interest to note that for this case, there is a slight initial rise in gasket pressure just inboard of the bolt line; this is a consequence of the pivot point initially being inboard of the bolt line.

Values for Flange Bending Stress for Preceding Simulations. In Table 2, we summarize the values obtained for flange bending stress at the maximum pressure obtained. The flange bending stress is computed using beam theory, with maximum bending moment computed from equilibrium equations once the current gasket state is established.

Table 2 Maximum stress in flange at final pressure

$\sigma_A = 6.895 \times 10^3$ kPa (1000 psi)

Prestrain, percent	Final pressure p/σ_A	Flange stress σ/σ_A
50.3	0.150	26.757
42.4	0.143	24.679
37.2	0.103	17.928
29.2	0.063	10.915
47.3 (smaller bolt diameter)	0.123	21.393

Effect of Rotational Resistance of Adjacent Structure. The simulations to this point have assumed that rotational resistance of the adjacent structure is negligible ($C = 0$ in equation (7)). We now simulate a configuration having rotational spring constant C consistent with a flat wall, cantilevered 50.8 cm (20 in.) away from the flange centerline and having thickness of 1.91 cm (0.75 in.). Fig. 4 shows results of this run using an initial prestrain of 47.1 percent and using the undersized bolts. The curve indicates the anticipated trend; the wall rotational resistance acts to inhibit flange rotation and raises final leakage pressure to 982.5 kPa (142.5 psi).

The results of this particular simulation verify that in a system which is experiencing leakage during initial shop hydrotest, the problem may be alleviated by adding stiffening to the adjacent pressure vessel wall. The addition of structure in this area may sufficiently decrease flange rotation so as to permit the unit to function without leakage failure. It must be noted, however, that the bolting is still overstressed in this case; even if the unit operates without leakage, the design cannot be deemed acceptable.

Effect of Gasket Simulation by Linear Spring Rates. For the final numerical simulation of this illustrative study, we return to the configuration using the larger bolt size (in order to eliminate the bolt overstress) and focus attention on the effects of simulating the gasket behavior by linear spring rates. Two linear simulations are modelled and applied to the case shown on Fig. 4 having initial gasket prestrain equal to 42.4 percent. Fig. 3 shows the linear simulation of loading behavior employed. The first simulation attempts to model some kind of an "average slope" and includes the origin and the point (0.525, 3.1,) on Fig. 3. The second simulation includes the origin and the point (0.425, 1.6) on Fig. 3 and attempts to insure that the gasket stress will nearly match the

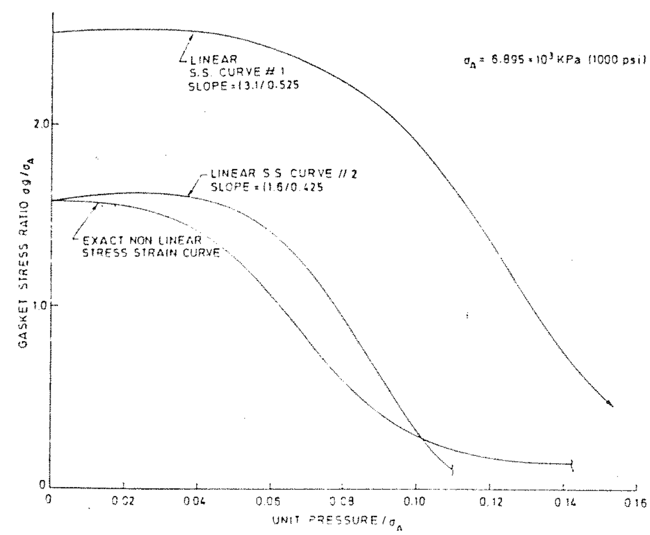

Fig. 5 Effect of gasket nonlinear behavior on leakage pressure

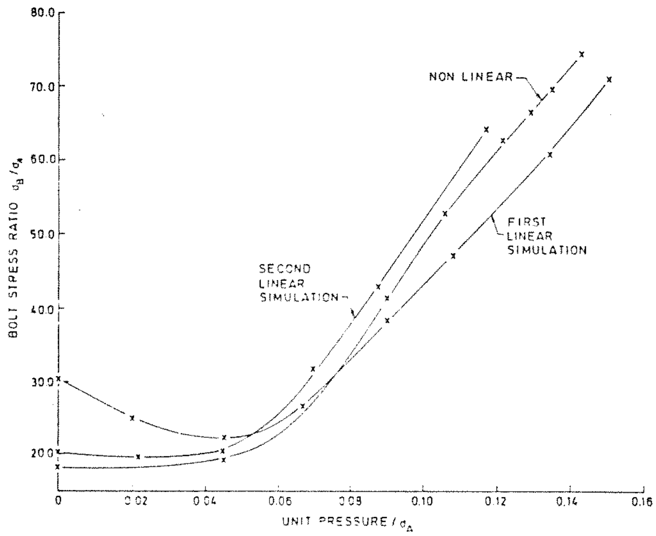

Fig. 6 Bolt stress versus pressure in unit

value obtained (using the true nonlinear stress strain curve) just prior to pressurization. Fig. 5 compares the results of the true nonlinear model and the two linear simulations. Once the results are obtained, the effects of a linear simulation are quite clear. The first linear simulation predicts that the ultimate leakage pressure will be considerably in excess of 1.034 kPa (150 psi). We can say that this nonconservative result is due to the gasket prestress level being considerably higher than the true nonlinear curve predicts when pressurization begins. The second linear simulation, while giving a good match with initial prestress level, predicts a considerably lower leakage pressure. This can be attributed to the fact that during pressurization, the gasket outboard of the bolt line does not offer as much resistance at the same strain level as does the true nonlinear case. The results of Fig. 5 show that for a full face gasket having nonlinear stress strain characteristics, an attempt at a linear simulation will generally lead to considerable error in the prediction of leakage pressure. Fig. 6 shows a plot of maximum bolt stress as a function of pressure for the three cases just discussed. As in Fig. 5, there is a considerable difference in the predicted behavior. The above results imply that at least for full face gaskets, accurate simulation of the nonlinear behavior is required if realistic results are to be obtained.

Comparisons with Finite Element and Full-Scale Tests

In order to assess the accuracy and efficiency of the method, a typical flange gasket configuration has been modelled using a large-scale commercial finite element program. Plane stress elements are used for the flange, while spring elements with nonlinear behavior and gap capability are used to model the gasket. An incremental solution procedure is employed within the finite element code. Using a realistic model of a full-scale unit, both the finite element code results and the special purpose code developed here yield leakage results within 8 percent of the actual behavior observed in a shop hydrotest. Whereas the unit was designed for test at 524 kPa (75 psi), actual shop testing indicated leakage at 384 kPa (55 psi). Both the finite element code and the program discussed herein not only agreed with each other within an expected accuracy, but also indicated failure by leakage at about 356 kPa (51 psi). It is of interest to note that the code discussed here was then immediately employed to examine proposed modifications to resolve the hydrotest leakage problem.

Conclusions

A method is proposed for simulating flange gasket behavior in a pressurized joint. Nonlinearity of the gasket material is accounted for in a realistic manner. The proposed method is capable of examining joint structural integrity, as well as leak tightness of the gasket. Numerical results have been presented which show the effect of gasket prestrain, wall flexibility, and bolt size on the final configuration. A comparison of nonlinear and linear gasket models indicates that for the case of full face gaskets, accurate modelling of the nonlinear gasket behavior is required to insure reasonable accuracy of the predictions.

The simulation employed here is ideally suited for incorporation into an optimization program which would automatically evolve candidate configurations that meet service stress and leakage requirements.

Acknowledgments

The author acknowledges the support of Ecolaire Condenser, Inc., during the development of this work, especially Mr. Robert Boyer and Mr. John Martin.

References

1 ASME Boiler and Pressure Vessel Code, Section III, Subsection NA, ASME, New York, 1974.

2 Waters, E. O., et al., "Formulas for Stresses in Bolted Flange Connections," *Transactions of the ASME*, Vol. 59, 1937, pp. 161-169.

3 Schneider, R. W., "Flat Face Flanges with Metal-to-Metal Contact Beyond the Bolt Circle," ASME *Journal of Engineering for Power*, Vol. 90, No. 1, Jan. 1968, pp. 82-88.

4 Waters, E. O., and Schneider, R. W., "Axisymmetric Nonidentical Flat Face Flanges with Metal-to-Metal Contact Beyond the Bolt Circle," ASME *Journal of Engineering for Industry*, Vol. 91, No. 3, Aug. 1969, pp. 615-622.

5 Gill, S. S., *Stress Analysis of Pressure Vessels and Pressure Vessel Components*, Chap. 6 ("Flanges" by R. T. Rose), Pergamon, New York, 1970, pp. 267-315.

6 Singh, K. P., "Study of Bolted Joint Integrity and Inter-Tube Pass Leakage in U-Tube Heat Exchangers," ASME Paper Nos. 77-WA/NE-6 and 7.

7 Stevens-Guille, P. D., and Crago, W. A., "Application of Spiral Wound Gaskets for Leak Tight Joints," ASME JOURNAL OF PRESSURE VESSEL TECHNOLOGY, Vol. 97, No. 1, Feb. 1975, pp. 29-33.

8 Swick, R. H., "How Much Pressure Will That Gasket Take?," *Machine Design*, Nov. 24, 1977, pp. 86-89.

9 Biot, M. A., *Mechanics of Incremental Deformations*, Wiley, 1965, Chaps. 2, 3, pp. 496-497.

APPENDIX

Simulation of Unloading Behavior in Gasket

As an application, we consider the data and results shown in Fig. 3. A plot of the experimental loading curve on semi-log paper indicates that the exponential behavior is reasonably simulated by

$$R = \frac{\sigma}{\sigma_A} = 0.1 e^{6.5\epsilon}; \quad \sigma_A = 6.895 \times 10^3 \text{kPa} \ \ (1000 \text{ psi}) \tag{31}$$

Using equation (18), we find that

$$\frac{\sigma_o}{\sigma_A} = 0.1; \quad \epsilon_1 = 0.154; \quad E = 12.17 \times 10^3 \text{ kPa} \tag{32}$$

suppose we now unload from the state $\sigma_f/\sigma_A = 6$, $\epsilon_f = 0.63$. Assuming $k = 9$, and estimating $(dR/d\epsilon)_f$ from the experimental data, yields

$$(dR/d\epsilon)_f = 140; \quad n = 16.22 \tag{33}$$

therefore, for unloading from $\epsilon_f = 0.63$, the analytical formulation, equation (19), becomes:

$$\frac{\sigma}{\sigma_A} = R = 6\left[0.1\left(\frac{\epsilon}{0.63}\right) + 0.9\left(\frac{\epsilon}{0.63}\right)^{16.22}\right] \tag{34}$$

If unloading occurs from the point $\sigma_f/\sigma_A = 1.6$, $\epsilon_f = 0.425$, then using the same values for $(dR/d\epsilon)_f$ and k, we obtain $n = 41.2$ and equation (19) becomes

$$\frac{\sigma}{\sigma_A} = R = 1.6\left[0.1\left(\frac{\epsilon}{0.425}\right) + 0.9\left(\frac{\epsilon}{0.425}\right)^{41.21}\right] \tag{35}$$

Equations (34), (35) are plotted on Fig. 3; it appears that a somewhat improved fit of the unloading behavior would be obtained by increasing $(dR/d\epsilon)_f$.